
STATE-OF-CHARGE ESTIMATION OF A LI-ION BATTERY USING DEEP FORWARD NEURAL NETWORKS

A PREPRINT



Alexandre Barbosa de Lima

Polytechnic School of the University of São Paulo
Department of Energy and Automation
alexandreblima@usp.br

Maurício B. C. Salles

Polytechnic School of the University of São Paulo
Department of Energy and Automation
mausalles@usp.br

José Roberto Cardoso

Polytechnic School of the University of São Paulo
Department of Energy and Automation
jose.cardoso@usp.br

September 22, 2020

ABSTRACT

This article presents two Deep Forward Networks with two and four hidden layers, respectively, that model the drive cycle of a Panasonic 18650PF lithium-ion (Li-ion) battery at a given temperature using the K-fold cross-validation method, in order to estimate the State of Charge (SOC) of the cell. The drive cycle power profile is calculated for an electric truck with a 35kWh battery pack scaled for a single 18650PF cell. We propose a machine learning workflow which is able to fight overfitting when developing deep learning models for SOC estimation. The contribution of this work is to present a methodology of building a Deep Forward Network for a lithium-ion battery and its performance assessment, which follows the best practices in machine learning.

Keywords Electrical Energy Storage · Li-ion battery · State-Of-the-Charge · Deep Learning · Artificial Intelligence

1 Introduction

1.1 State of the Art and Trends in Li-ion Battery Estimation

Energy storage acts as a mediator between variable loads and variable sources. Electricity storage is not new. Volta invented the modern battery in 1799. Batteries were implemented in telegraph networks in 1836 [1]. The Rocky River Hydroelectric Power Plant in New Milford, Connecticut, was the first major electrical energy storage (EES) system project in the United States. The plant used hydroelectric storage technology through Pumped Hydroelectric Storage (PHS) pumping.

This research is motivated by the study of the application of EES systems in the area of sustainable energy sources.

Hannan et al. [2] present a detailed taxonomy of the types of energy storage systems taking into account the form of energy storage and construction materials: mechanical, electrochemical (rechargeable and flow batteries), chemical, electrical (ultracapacitor or superconducting magnetic coil), thermal and hybrid.

Recently, industry and academia have given great importance to the electrification of the transport system, given the need to reduce the emission of greenhouse gases. Hybrid electric vehicles, such as the Toyota Prius, or fully electric vehicles, such as the various Tesla models, the Nissan Leaf and the GM Volt, are successful cases in the United States [3].

The advancement of EES technologies enabled the emergence of the iPod, smartphones and tablets with lithium-ion (li-ion) batteries. If renewable sources, such as solar and wind, become prevalent, the EES will be one of the critical

components of the electricity grid, given the intermittent nature of these energy sources [3, 4]. EES systems are necessary even when renewable sources are connected to the grid, because it is necessary to smooth the energy supply. For example, the EES of a building or factory can be charged during hours of reduced demand and supply/supplement energy demand during peak hours.

EES technology consists of the process of converting a form of energy (almost always electrical) to a form of storable energy, which can be converted into electrical energy when necessary. EES has the following functions: to assist in meeting the maximum electrical load demands, to provide time-varying energy management, to relieve the intermittency of renewable energy generation, to improve energy quality/reliability, to serve remote loads and vehicles, to support the realization of smart grids, improve the management of distributed/standby power generation and reduce the import of electricity during peak demand periods [4, 5].

An EES (which can connect to the network or operate in stand-alone mode) consists of two main subsystems: i) storage and ii) power electronics. Such subsystems are complemented by other components that include monitoring and control systems [1].

Lithium-ion battery technology has attracted the attention of industry and academia for the past decade. This is mainly due to the fact that lithium-ion batteries offer more energy, higher power density, higher efficiency and lower self-discharge rate than other battery technologies such as NiCd, NiMH, etc. [6].

The efficient use of the lithium-ion battery requires the supervision of a Battery Management System (BMS), as it is necessary that the battery operates under appropriate conditions of temperature and charge (State-Of-Charge (SOC)) [7]. The cell temperature produces deleterious effects on the open circuit voltage, internal resistance and available capacity and can also lead to a rapid degradation of the battery if it operates above a given temperature threshold. Therefore, the modeling of the battery is of paramount importance, since it will be used by the BMS to manage the operation of the battery [6].

There are two methods of battery modeling: i) model-driven and ii) data-driven (based on data that is collected from the device) [8].

Electrothermal models, which belong to the category of model-driven methods, are commonly classified as: i) electrochemical or ii) based on Equivalent Circuit Models (ECM) [6, 7].

Electrochemical models are based on partial differential equations [9] and are able to represent thermal effects more accurately than ECM [10]. However, the first class of models requires detailed knowledge of proprietary parameters of the battery manufacturer: cell area, electrode porosity, material density, electrolyte characteristics, thermal conductivity, etc. This difficulty can be eliminated by characterizing the battery using a thermal camera and thermocouples. But this solution is expensive, time consuming and introduces other challenges such as the implementation of dry air purge systems, ventilation, security, air and water supply, etc. Electrochemical models demand the use of intensive computing systems [7].

On the other hand, the ECM-based approach has been used for computational/numerical analysis of batteries [7]. In this case, the objective is to develop an electrical model that represents the electrochemical phenomenon existing in the cell. The level of complexity of the model is the result of a compromise between precision and computational effort. Note that an extremely complex and accurate ECM may be unsuitable for application in embedded systems.

The most recent literature show that the machine learning approach, based on deep learning algorithms is the state of the art in the area [8, 11–20]. Machine learning is a branch of AI, as will be seen in section 2.

Chemali et al [12] compared the performance of Deep Neural Networks (DNN) with those of other relevant algorithms that have been proposed since the second half of the 2000s. The article shows that the SOC estimation error obtained with deep learning is less than the following methods:

- Model Adaptive-Improved Extended Kalman Filter (EKF) [21];
- Adaptive EKF with Neural Networks [22];
- Adaptive Unscented Kalman Filter (AUKF) with Extreme Machine Learning [23];
- Fuzzy NN with Genetic Algorithm [24]; and
- Radial Bias Function Neural Network [25].

Estimating the SOC of lithium ion cells in a BMS by means of deep learning offers at least two significant advantages over model driven approaches, namely: i) neural networks are able to estimate the non linear functional dependence that exists between voltage, current and temperature (observable quantities) and unobservable quantities, such as SOC, with great precision and ii) the problem of identifying ECM parameters is avoided.

1.2 Contribution of the paper

In relation to the literature already mentioned, this paper takes a step back as far as reasons related to the methodology adopted for the construction and performance measurement of a deep learning model are concerned.

First, we work with Deep Feedforward Networks (DFN) as a baseline family model, as they form the basis of many important commercial applications [14]. Our preliminary results show that a simple architecture with four hidden layers is already quite interesting. We do not work with Recurrent Neural Networks (RNN) because they are suitable for sequential data processing problems such as machine translation.

Second, the central challenge in machine learning is that our model has to perform well on new, unseen inputs, not just those on which our algorithm was trained. This ability is called generalization. What separates machine learning from traditional optimization is that we want the generalization error, or test error, to be as low as possible [14]. To do this, we need a test set. In this work we followed the best practice of breaking the test set into two separate sets: validation and test sets [26]. That is, the generalization power of the models were measured against validation and test sets. The validation set is used to fine tune the network hyperparameters.

Third, as a corollary of generalization, the central problem in machine learning, namely overfitting, has not been properly addressed, to the best of our knowledge, in the recent mainstream literature of SOC estimation of Li-ion batteries using deep learning. Thus, we have to apply concepts from statistical learning theory [14]. Overfitting occurs when the gap between the training error and generalization error is too large. The processing of mitigating overfitting is called regularization, which can be defined as any modification we make to a learning algorithm with the goal of reducing its generalization error but not its training error. To see this phenomenon, one has to plot the training and generalization learning curves, see Fig. 1 for instance.

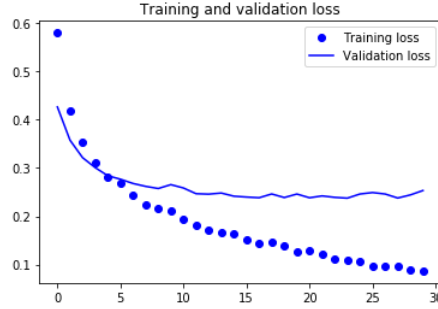


Figure 1: Training and generalization errors behave differently. The horizontal axis represents the number of epochs. The vertical axis is the loss function. Note that the model starts to overfit around the fifth epoch.

Note that the literature of machine learning presents a solid framework for solving deep learning problems, such as model evaluation and the attack on overfitting, among others [14, 26, 27]. The satisfactory result obtained in this article in terms of a low generalization error takes overfitting into account.

Fourth, as mentioned before, we have to consider the optimization problem in the context of deep learning, which completely differs from traditional optimization algorithms in several ways. In this work, we use algorithms with adaptive learning rules, such as RMSProp and Adam, which include the concept of momentum, allowing faster convergence than Stochastic Gradient Descent (SGD), at the cost of more computation. The learning rate is one of the most difficult hyperparameters of a artificial neural network (ANN) to be configured as it significantly affects the model performance. Note that small values of the learning rate result in a slow convergence of deep learning. On the other hand, if the learning rate is too large, gradient descent can overshoot the minimum. It may fail to converge, or even diverge.

Fifth, the validation error is estimated by taking the average validation error across K trials. We use a simple, but popular solution, called K -fold cross-validation (Fig. 2), which consists of splitting the available training data into two partitions (training and validation), instantiating K identical models, for each fold $k \in \{1, 2, \dots, K\}$, and training each one on the training partitions, while evaluating on the validation partition. The validation score for the model used is then the average of the K validation scores obtained. This procedure allows network hyperparameters to be adjusted so that overfitting is mitigated [27, p. 23]. It is usual to use about 80% of the data for the training set, and 20% for the validation set. Note that the validation scores may have a high variance with regard to the validation split. Therefore, K -fold cross-validation help us improve the reliability when evaluating the generalization power of the model.

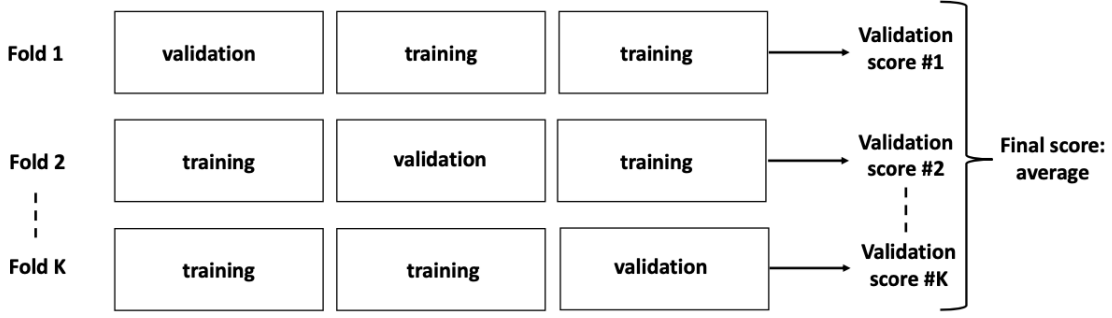


Figure 2: K-fold cross-validation.

1.3 Organization of the paper

The remainder of the paper is organized as follows. Section 2 presents an overview of AI, machine learning and deep learning for the reader who is not familiar with the subject. Section 3 presents our experimental results. Finally, section 4 presents our conclusions.

2 Artificial Intelligence and Deep Learning

2.1 The Notion of Neural Nets

The Handbook of Artificial Intelligence presents the following operational definition¹ for Artificial Intelligence (AI) [28]:

“Artificial Intelligence (AI) is the part of computer science concerned with designing intelligent computer systems, that is, systems that exhibit the characteristics we associate with intelligence in human behavior - understanding language, learning, reasoning, solving problems, and so on”.

There are two main lines of research in AI: the connectionist and the symbolic. According to Boden [29], both were inspired by the seminal article entitled *A Logical Calculus of the Ideas Immanent in Nervous Activity* (1943), by Warren Sturgis McCulloch and Walter Pitts [30], the first modern computational theory². The literature recognizes that the research carried out by McCulloch and Pitts is the pioneering work in AI [32].

Fig. 3 illustrates the McCulloch and Pitts artificial neuron model.

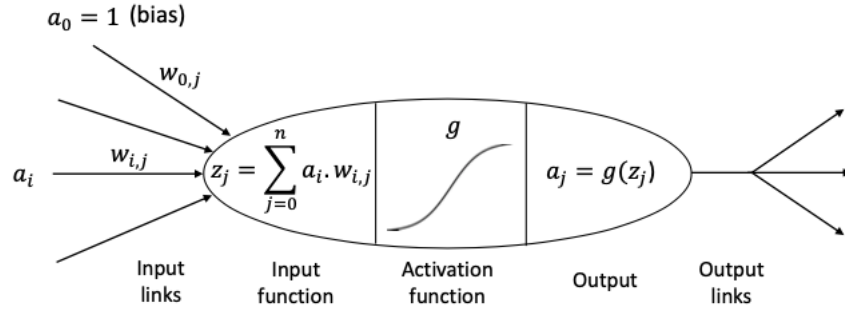


Figure 3: McCulloch and Pitts model

¹There is no consensus on the concept of intelligence.

²The theory is considered modern because it employs the mathematical notion of computation established by Turing in 1936 [31].

The artificial neuron (or unit) of Fig. 3 has the following characteristics:

- input signals (activations) (a_1, a_2, \dots, a_n) are 0 or 1 bits. The external signal $a_0 = 1$ is known as the bias³;
- synaptic weights of the j -th neuron: w_0, w_1, \dots, w_n ; and
- a_j denotes the output signal (or output activation) of the j th neuron, given by

$$z_j = \sum_{i=0}^n w_{i,j} a_i \quad (1)$$

$$a_j = g(z_j) = \{0, 1\} \quad (2)$$

where $z = f(a)$ is the input function and $g(z)$ is a nonlinear activation function. The output is binary (bit 0 or bit 1); therefore, the McCulloch and Pitts model is said to have the “all or nothing” property.

The activation function of the McCulloch and Pitts model is the Heaviside function (unit step function)

$$g(z) = \begin{cases} 1, & z \geq 0 \\ 0, & z < 0 \end{cases} \quad (3)$$

$g(z) = 1$ se $z \geq 0$ ou $g(z) = 0$ para $z < 0$.

We take the opportunity to make a necessary digression on the neuron model of Fig. 3, in order to present the intuition behind the fact that modern ANN (see Fig. 4) are able to approximate nonlinear functions with arbitrary precision, at least in theory (universal approximation theorem [33]). The explanation below considers a network with only one layer of $N + 1 = M$ neurons in parallel, where each neuron is excited by the input signal $\mathbf{a} = \{a_0, a_1, \dots, a_N\}$, not necessarily binary. This layer is known as the hidden layer.

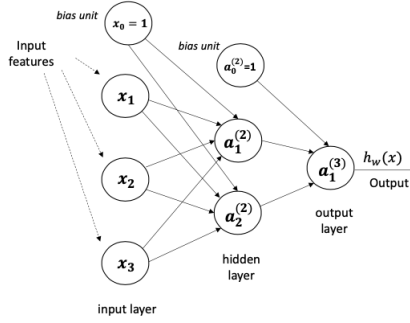


Figure 4: Example of a densely connected neural net with one hidden layer. The hidden layer has three units ($a_0^{(2)}$, $a_1^{(2)}$, and $a_2^{(2)}$). The input features are the input signals \mathbf{x} . The function $\mathbf{y} = \mathbf{h}_w(\mathbf{x})$ is called the model or hypothesis.

Let’s rewrite (1) in a vectorized form

$$z_i = \mathbf{W}^T \mathbf{a} \quad (4)$$

where we adopt the notation \mathbf{W} for the vector of synaptic weights, \mathbf{a} for the vector of entries and T denotes the transposition of matrices⁴.

Consider the Discrete Fourier Transform (DFT)⁵ of an input signal $\mathbf{b} = \{b_0, b_1, \dots, b_N\}$ given by

$$B[k] = \begin{cases} \sum_{i=0}^N (e^{-j2\pi \frac{k}{M} i}) b_i, & 0 \leq k \leq N \\ 0, & \text{otherwise} \end{cases} \quad (5)$$

³The bias plays the role of the intercept b in the simple linear regression model $y = wx + b$.

⁴This article assumes that vectors are always column vectors, as it is usual in the signal processing area.

⁵The imaginary unit is represented by j .

and the corresponding inverse transformation, called Inverse Discrete Fourier Transform (IDFT) [34]

$$z_i = \begin{cases} \sum_{k=0}^N (\frac{1}{M} e^{j2\pi \frac{k}{M} i}) B[k], & 0 \leq k \leq N \\ 0, & \text{otherwise} \end{cases} \quad (6)$$

Rewriting (6) in vectorized form, we obtain

$$z_i = \mathbf{W}^T \mathbf{B} \quad (7)$$

where $\mathbf{W} = \{(\frac{1}{M} e^{j2\pi \frac{k}{M} i})\}, 0 \leq k \leq N$, and $\mathbf{B} = \{B_0, B_1 \dots B_N\}$.

Compare (7) and (4). Note that these equations are equal if $\mathbf{a} = \mathbf{B}$. Therefore, Eq. (7) suggests that it would be possible to represent the function $z = f(a)$ through a neural network that uses the weights $\{\frac{1}{M} e^{j2\pi \frac{k}{M} i}\}, 0 \leq k \leq N$. Eq. (7) looks like a Fourier series.

Remember that Fourier showed in 1807 that an arbitrary and aperiodic function $f(t)$ defined in a finite interval T_0 can be reconstructed from a trigonometric series called the Fourier series [35]. So “there is nothing new under the sun”. Electrical engineers are well familiarized with this notion.

As mentioned before, the universal approximation theorem states that a feedforward network with a linear input and at least one hidden layer of artificial units with an non linear activation function can approximate any “function”⁶ from one finite-dimensional space to another with any desired nonzero amount of error, provided that the network is given enough units [14, 33]. However, the theorem does not say what the number of units in the hidden layer should be. We also have no guarantees that the training algorithm will be able to learn that function. This may be due to the existence of local minimums in the cost function to be optimized.

Nowadays, the activation function called REctified Linear Unit (Relu) (see Fig5), given by

$$g(z) = \max\{0, z\} \quad (8)$$

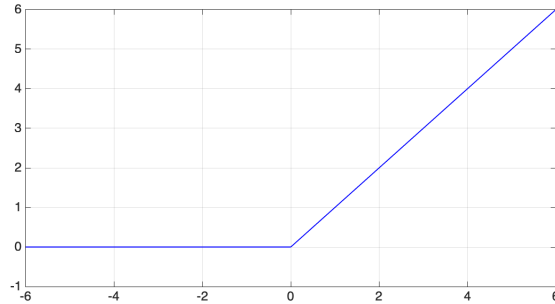


Figure 5: Relu activation function.

is commonly used in ANN [14].

An ANN is a distributed parallel processing system, inspired by the processing structure of the human brain. The ANN technique is a form of non-algorithmic computation of functions.

The connectionist approach uses ANN. The symbolic line, sometimes called the symbolic AI (“Good Old Fashioned AI (GOFAI) [29]) follows the logical tradition and had John McCarthy and Allen Newell, among others, as some of its great exponents [36].

Since 2006, the connectionist line has gained prominence, due in large part to the fundamental contributions of the researchers Yoshua Bengio, Geoffrey Hinton, and Yann LeCun, who were awarded the 2018 A. M. Turing Award [37]. Nowadays AI research is dominated by systems that use ANN, also known as Deep Learning [14]. Fig. 7 shows a deep learning model for handwritten digit recognition (a classical problem in computer vision), first solved by LeCun et al [38]. The model has one input layer, four hidden layers, and one output layer.

⁶In fact, any Borel function. This concept is beyond the scope of this paper and will not be discussed.

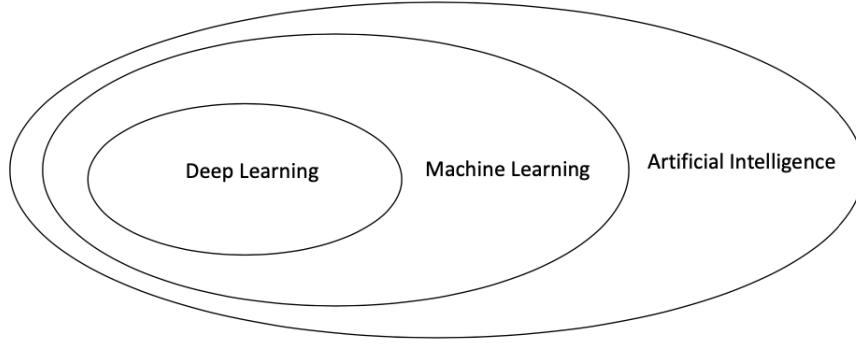


Figure 6: Relationship between AI, machine learning and deep learning.

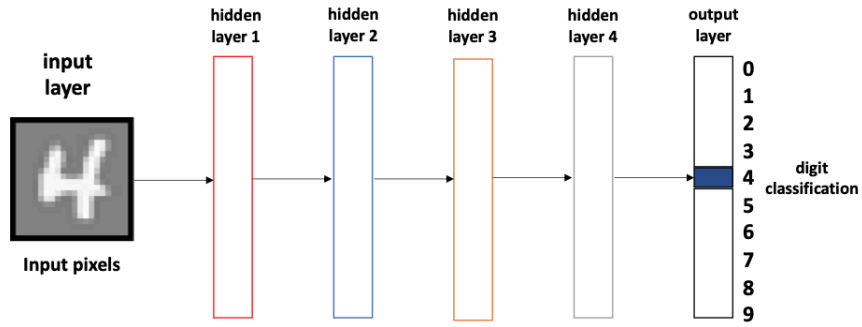


Figure 7: Handwritten Digit Recognition with a 6 layers ANN.

2.2 Machine Learning

Starting at 1952, Arthur Samuel, the pioneer of machine learning in the era of digital computers [39], wrote a series of programs for IBM computers that learned to play checkers⁷ through a learning process that was not based on neural networks. The program was shown on TV at 1956, making a strong impression on public opinion [40, 41].

Tom Mitchell gives a definition of machine learning [42, p. 2]

“A computer is said to **learn** from experience E with respect to some class of tasks T and performance measure P , if its performance at tasks in T , as measured by P , improves with experience E ”.

As Samuel have shown, checkers is a problem that can be solved using machine learning algorithms. According to Mitchell’s definition, we have that:

- E = “training” of the program, which consists of the program playing a sufficiently large number⁸ of checkers games against itself.
- T = playing games.
- P = percent of games won against opponents.

Machine learning algorithms can be divided into four groups [26]:

- **Supervised Learning:** in which the man provides the input data (training set), as well as the expected responses from the data (a label is attached to each data). The output of the processing is a set of rules, which will be applied on new input data, in order to produce original responses (inferences of the classification or regression type).

⁷The work was developed during Samuel’s free time.

⁸For example, hundreds of thousands of games.

- **Unsupervised Learning:** for training a descriptive model capable of recognizing patterns. There is no teacher. Applications: discover shopping patterns in supermarkets and data clustering tasks (eg, identifying groups of people who share common interests such as sports, religion or music).
- **Self-supervised Learning:** is a type of supervised learning; there are still labels involved (because learning needs to be supervised by something), but they are generated from the input data, usually using a heuristic algorithm.
- **Reinforcement Learning:** a program is trained to interact in a environment through actions to achieve a goal. Learning uses a rewards and/or punishment mechanism. The AlphaZero algorithm⁹, developed by Google DeepMind, uses this technique [43].

Supervised learning, which is used in this work, involves the training of a model or hypothesis. To this end, given a set of training data (or training set), the learning algorithm aims to fit a model that minimizes a metric of choice.

In 1959, Bernard Widrow and Martian E. Hoff discovered the famous machine learning algorithm called Least Mean Square (LMS) [44]. The LMS algorithm belongs to the family of stochastic gradient algorithms and uses the method of optimization of the gradient descent, which is also used in deep learning, whose objective is to find the values of the parameters that minimize a given function, called objective function or cost function.

Adaline implements supervised machine learning, since the desired response for each input pattern is provided.

In 1958, Frank Rosenblatt presented the theory of a hypothetical nervous system called the Perceptron [45]. Perceptron is a single-layer ANN with a learning rule capable of implementing a linear classifier.

A Perceptron follows the feed-forward processing model, from left (inputs) to right (output (s)).

The 1980s were marked by the discovery of the backpropagation algorithm, which updates the gradient for multilayer networks [46]. The wide dissemination of the results in the collection *Parallel Distributed Processing* [46], edited by Rumelhart and McClelland, caused great excitement in the areas of Computer Science and Psychology.

In fact, the backpropagation algorithm was discovered independently several times [47–50].

2.3 Statistical Learning

This section introduces a very short review of the main concepts about stochastic processes (also called data-generating processes by the literature of deep learning [14]) and statistical learning that are used in this paper. The purpose is just to indicate what is important to be known without entering into the details. The interested reader should refer to the appropriate literature [27, 51].

Definition 2.3.1 (Stochastic Process). *Let T be an arbitrary set. A stochastic process is a family $\{\mathbf{x}_t, t \in T\}$, such that, for each $t \in T$, \mathbf{x}_t is a random variable.* ■

When the set T is the set of integer numbers \mathbb{Z} , then $\{\mathbf{x}_t\}$ is a discrete time stochastic process (or random sequence); $\{\mathbf{x}_t\}$ is a continuous time stochastic process if T is taken as the set of real numbers \mathbb{R} .

The random variable \mathbf{x}_t is, in fact, a function of two arguments $\mathbf{x}(t, \zeta)$, $t \in T$, $\zeta \in \Omega$, given that it is defined over the sample space Ω . For each $\zeta \in \Omega$ we have a realization, trajectory or time series x_t . The set of all realizations is called ensemble. Each trajectory is a function or a non-random sequence and for each fixed t , x_t is a number.

A process \mathbf{x}_t is completely specified by its *finite-dimensional distributions* or n -order probability distribution functions, as:

$$F_{\mathbf{x}}(x_1, x_2, \dots, x_n; t_1, t_2, \dots, t_n) = P\{\mathbf{x}(t_1) \leq x_1, \mathbf{x}(t_2) \leq x_2, \dots, \mathbf{x}(t_n) \leq x_n\} \quad (9)$$

in which t_1, t_2, \dots, t_n are any elements of T and $n \geq 1$.

The first order probability distribution function is also known as Cumulative Distribution Function - CDF.

The *probability density function* - PDF is given by:

$$f_{\mathbf{x}}(x_1, x_2, \dots, x_n; t_1, t_2, \dots, t_n) = \frac{\partial^n F_{\mathbf{x}}(x_1, x_2, \dots, x_n; t_1, t_2, \dots, t_n)}{\partial x_1 \partial x_2 \dots \partial x_n}. \quad (10)$$

⁹AlphaZero defeated the world champion of Go, Lee Sedol, in a challenge sponsored by Google in 2016 in South Korea.

Applying the conditional probability density formula,

$$f_{\mathbf{x}}(x_k | x_{k-1}, \dots, x_1) = \frac{f_{\mathbf{x}}(x_1, \dots, x_{k-1}, x_k)}{f_{\mathbf{x}}(x_1, \dots, x_{k-1})}, \quad (11)$$

in which $f_{\mathbf{x}}(x_1, \dots, x_{k-1}, x_k)$ denotes $f_{\mathbf{x}}(x_1, \dots, x_{k-1}, x_k; t_1, \dots, t_{k-1}, t_k)$, repeatedly over $f_{\mathbf{x}}(x_1, \dots, x_{n-1}, x_n)$ we get the probability chain rule

$$f_{\mathbf{x}}(x_1, x_2, \dots, x_n) = f_{\mathbf{x}}(x_1) f_{\mathbf{x}}(x_2 | x_1) f_{\mathbf{x}}(x_3 | x_2, x_1) \dots f_{\mathbf{x}}(x_n | x_{n-1}, \dots, x_1). \quad (12)$$

When \mathbf{x}_t is a sequence of *mutually independent* random variables, (12) can be rewritten as

$$f_{\mathbf{x}}(x_1, x_2, \dots, x_n) = f_{\mathbf{x}}(x_1) f_{\mathbf{x}}(x_2) \dots f_{\mathbf{x}}(x_n). \quad (13)$$

Definition 2.3.2 (Purely Stochastic Process). *A purely stochastic process $\{\mathbf{x}_t, t \in \mathbb{Z}\}$ is a sequence of mutually independent random variables.* ■

Definition 2.3.3 (IID Process). *An Independent and Identically Distributed (IID) process $\{\mathbf{x}_t, t \in \mathbb{Z}\}$, denoted by $\mathbf{x}_t \sim \text{IID}$, is a purely stochastic and identically distributed process.* ■

As mentioned earlier, the central challenge in machine learning is that the algorithm performs well on the test set. The training and test sets are generated by the same data-generating process. Typically, it is assumed that the examples in each set are independent and that the training and test sets are identically distributed. These assumptions are collectively known as IID.

The **no free lunch theorem** [52] says that, considering the average over all the possible data-generating processes, any machine learning algorithm has the same error rate when evaluated on previously unobserved examples. That is, there is not, at least in theory, a machine learning algorithm that is better than all others for all cases.

However, the no free lunch theorem is valid only when working with the average over all the possible data-generating processes. Fortunately, that does not happen in real life, as the physical data-generating process of a Li-Ion cell is a result of the restrictions imposed by the real world over all the possible data-generating processes. Thus, in practical applications, it is realistic to think about designing algorithms that have a good performance for a given Li-Ion cell.

Going further, the goal of research in machine learning is not to look for a universal learning algorithm. Instead, we have to understand what the stochastic characteristics of our dataset are, in order to design, validate and test an algorithm that is efficient for that specific data set.

2.4 ANN as Deep Learning

Interest in ANNs has resurfaced with the advent of the Deep Belief Nets in 2006 [53]. The work of Hinton, Osindero and Teh demonstrated that a type of DNN could be trained with high efficiency. Their research triggered the current wave of research in ANN, which popularized the term deep learning.

Deep learning denotes the idea of a neural network with multiple hidden layers that has the ability to partition the representation of an entry into multiple layers (see Fig.7). The number of layers in a model corresponds to the depth of the network [26].

The success of deep learning today is due to: i) the emergence of Big Data, which made it possible to store data for training in databases with tens of millions of examples, ii) the advent of Graphics Processing Unit (GPU), and iii) advances in algorithms.

Fig. 8 illustrates how deep learning works [26]. The variables \mathbf{x} and \mathbf{y} denote the input signal (training example) and the desired signal (target), respectively. The function $\mathbf{h}_{\mathbf{w}}(\mathbf{x})$ is the mathematical model or hypothesis. The estimation error (residual or loss score) is given by $\mathbf{e} = \mathbf{y} - \mathbf{h}_{\mathbf{w}}(\mathbf{x})$. At startup, random values are assigned to the \mathbf{w} weights of the network, so the value of the initial residue is high. However, in the course of processing the training examples, the weights are adjusted incrementally in the correct direction; at the same time, the value of the loss function decreases. This is the training loop, which, being repeated enough times, typically dozens of iterations over thousands of examples, produces weights that minimize the cost function. A network is considered trained when the minimum of the cost function is reached.

Deep learning has achieved the following advances, all in historically difficult areas of machine learning, such as [18,26]:

- nonlinear regression;
- superhuman image classification;

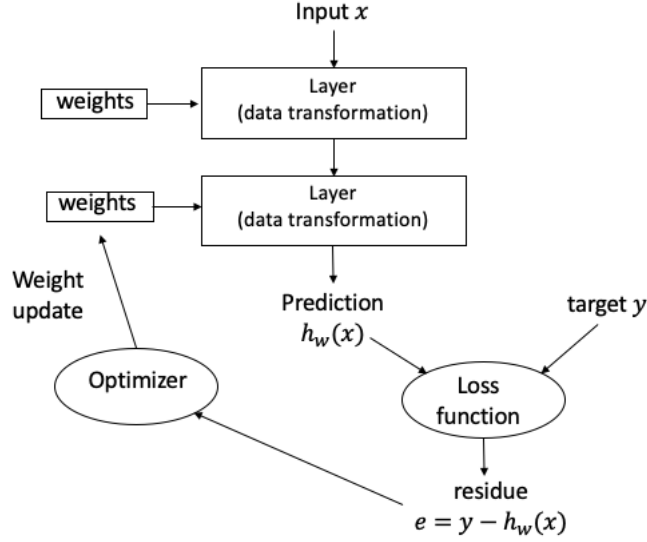


Figure 8: How deep learning works.

- voice recognition at an almost human level;
- transcription of almost human handwriting;
- automatic translation;
- text to speech conversion;
- autonomous vehicle driving at an almost human level; and
- superhuman performance in games like chess, shogi and Go.

However, deep learning has limitations. Current ANN architectures do not have the power to track statistical changes of the training data in real time. In other words, deep learning is not yet adaptive. Note that training a DNN at a dedicated workstation can take days or weeks. This is due to the computational complexity of deep learning.

Furthermore, the science of deep learning is not like mathematics or physics, in which theoretical advances can be achieved with a chalk and a blackboard. Deep learning is an engineering science [54], as it does not yet have a mathematical formalism like that of the area of adaptive filtering. For example, as we have stated before, there is no design criterion for the number of layers in the network, much less for the number of neurons in a hidden layer. The field is driven by experimental discoveries. But of course, there are best practices to be followed [26].

2.5 A Workflow for Approaching Deep Learning Problems

In this paper, we follow an adapted version of the supervised machine learning workflow proposed by Chollet (see Fig. 9) [26]:

1. Choose a reliable dataset. If you do not find a dataset, collect the data of interest, and annotate it with labels.
2. Choose how you will measure success on your problem. Which metrics will you monitor on your validation data?
3. Determine your evaluation protocol: K-fold cross-validation? Which portion of the data should you use for validation?
4. Develop a baseline model with statistical power.
5. Develop a model that overfits.
6. Regularize your model and tune its hyperparameters, based on performance on the validation data.

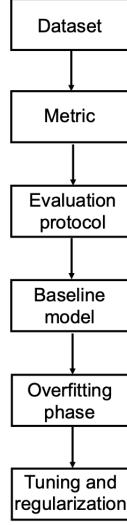


Figure 9: Deep learning workflow.

3 Experimental Results

3.1 Deep Learning Methodology and Modeling

We selected the 2.9 Ah Panasonic 18650PF Li-ion Battery Data provided by Dr. Phillip Kollmeyer, University of Wisconsin-Madison [55]. Note that this dataset has been used by some of the top works in the area [11, 12, 19, 20].

A series of nine drive cycles were made public, among them a Neural Network (NN) cycle, which is the cycle of our interest. More specifically, the simulations in this section present the results for data collected at a temperature of 25° C.

The NN drive cycle was designed to have some additional dynamics which are useful for training neural networks. The drive cycle power profile is calculated for an electric Ford F150 truck with a 35kWh battery pack scaled for a single 18650PF cell.

Fig. 10 shows the following 2.9 Ah Panasonic 18650PF Li-ion cell characteristic curves:

- temperature (° C) vs SOC (%);
- amp-hours discharged vs time (minutes);
- voltage (V) vs time (minutes);
- current (A) vs time (minutes);
- temperature (° C) vs time (minutes); and
- voltage (V) vs SOC (%).

The input data (\mathbf{x}) or features are: $x_1 = v(t)$ (voltage in V), $x_2 = i(t)$ (current in A), and $x_3 = T(t)$ (temperature in °C), where t denotes time in seconds. We see no reason for the inclusion of extra features in the hypothesis space, as the other data collected in [55] are: i) Wh (measured watt-hours, with Wh counter reset after each charge, test, or drive cycle), Power (measure power in watts), and Chamber-Temp-degC (measured chamber temperature in degrees Celsius). The output variable or target (y) is the SOC (%). The dataset has 116,982 examples, which were divided examples for training, validation, and testing, respectively.

We applied feature normalization on the input data using the formula

$$\mathbf{x}_{\text{normalized}} = \frac{\mathbf{x} - \mu_{\mathbf{x}}}{\sigma_{\mathbf{x}}} \quad (14)$$

where $\mu_{\mathbf{x}}$ and $\sigma_{\mathbf{x}}$ denote the mean and standard deviation of \mathbf{x} .

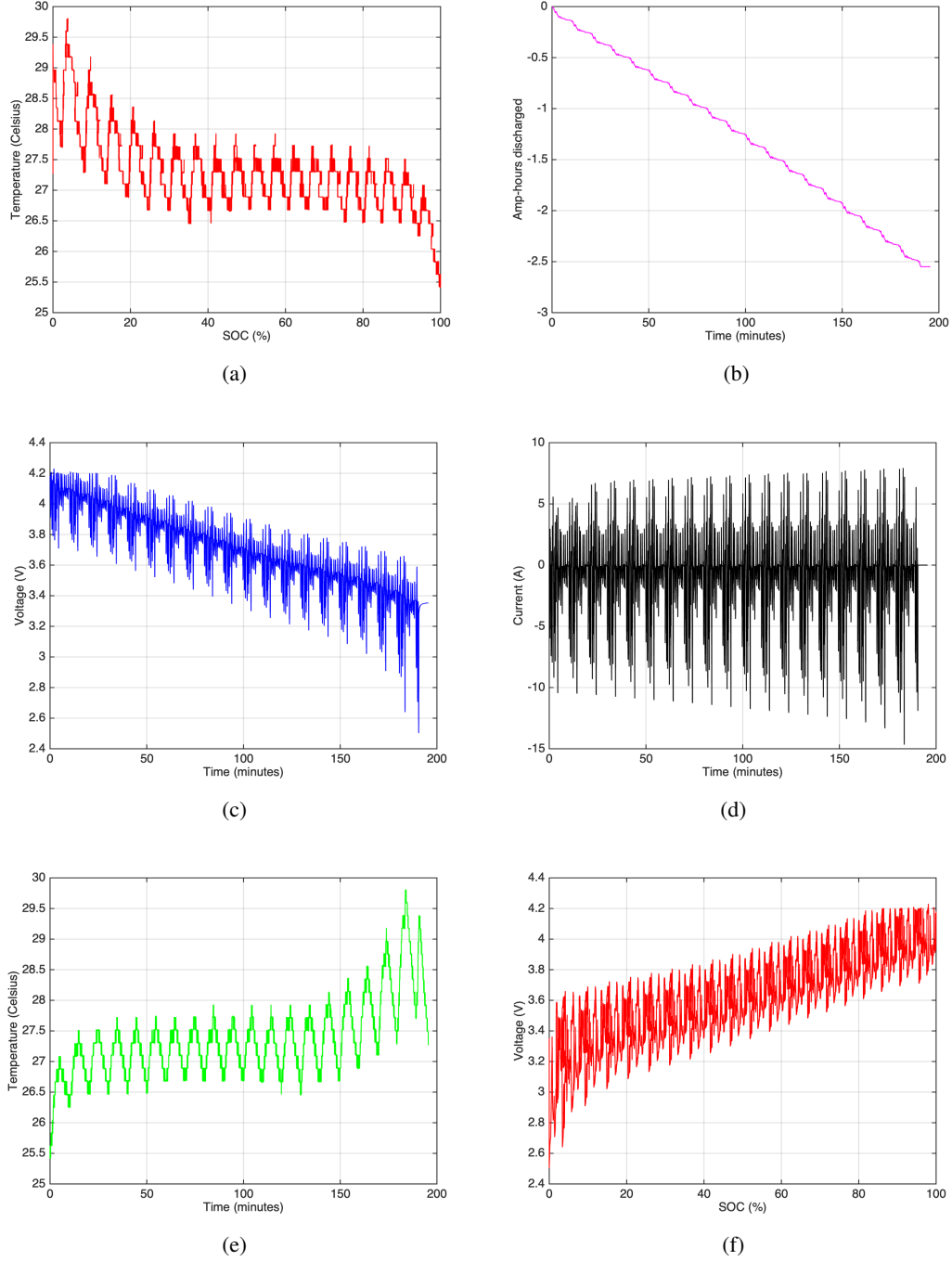


Figure 10: in (a), (b), (c), (d), (e), and (f) we have: temperature ($^{\circ}$ C) vs SOC (%), amp-hours discharged vs time (minutes), voltage (V) vs time (minutes), current (A) vs time (minutes), temperature ($^{\circ}$ C) vs time (minutes), and voltage (V) vs SOC (%), respectively.

We choose Mean Absolute Error (MAE) as the performance metric [12] and the K-fold cross-validation as the basic method to fight overfitting. Notwithstanding, we have also used weight regularizers and dropout layers with the same goal.

The literature review indicated that the Python language is the most suitable for this research, for it has several free and open source frameworks for deep learning. In addition, Python is the language most used by the machine learning community [26, 56, 57]. Other options like R also have great machine learning libraries [54].

Open source deep learning frameworks such as TensorFlow [58], PyTorch [59], MXNet [60] and Microsoft Cognitive Toolkit (CNTK) [61]¹⁰ have stood out in recent years. However, TensorFlow 2 and the Keras API offer some differentials, such as the possibility of executing codes in Google Collaboratory, or "Colab" [63], just using a browser and with free access to CPU/GPU (and even to Google's Tensor Processor Unit (TPU)).

In addition, TensorFlow offers a browser-based visualization tool called TensorBoard, whose main objective is to help the user visually monitor everything that happens inside their model during training [26]. TensorBoard automates some features such as visualizing the learning curve of neural networks.

Thus, we decided to use the Python language and the TensorFlow 2 framework in conjunction with the Keras API. We coded/prototyped the deep learning model in the Spyder IDE (Python 3.7) of the Anaconda package manager.

3.2 Tuning of Hyperparameters

Fig. 11 shows the architecture of a densely connected DFN with four (4) layers (two hidden layers). Fig. 12 shows the learning curves using Adam optimizer and 4-fold cross-validations. Note that overfitting manifests itself as a gap between the validation MAE (red plot) and the training MAE (blue plot) in those figures.

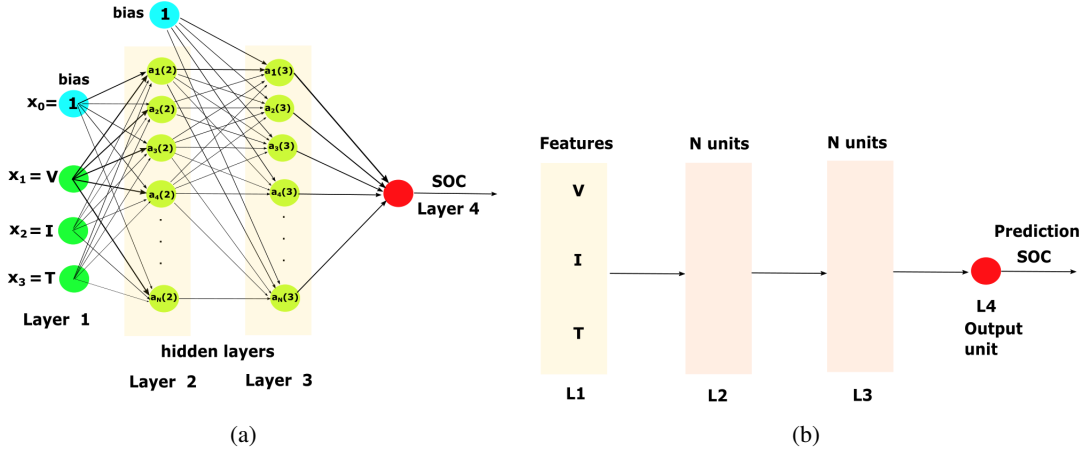


Figure 11: (a) and (b): densely connected 4-layer DFN and its schematic version, respectively.

We tuned the hyperparameters of the deep learning model using L^1/L^2 parameter norm penalties and adding two extra dropout layers.

In L^2 regularization, the cost added to the objective function is proportional to the square root of the sum of the square values of the weight coefficients (L^2 norm – $\|w\|_2^2$), whereas in L^1 regularization the cost added to the objective function is proportional to the sum of the absolute values of the weight coefficients (L^1 norm – $\|w\|_1$).

Fig. 13 shows the architecture of a DFN with six (6) layers, where we have, after the input layer (layer 1), in sequence, two pairs of a 256 units/hidden layer followed by a dropout layer, then the final layer. The neural net uses 8-fold cross-validations. In Fig. 14, note that overfitting occurs only around 35 epochs. Thus, this model has a greater power of generalization than the previous ones, as expected.

3.3 SOC Estimation Results

The DFN model with two hidden layers, 256 units/hidden layer, batch size of 128 and without regularization achieves the best SOC's estimate on the test set, with a MAE of approximately 1.60%.

¹⁰The Caffe2 [62] library has been absorbed by PyTorch.

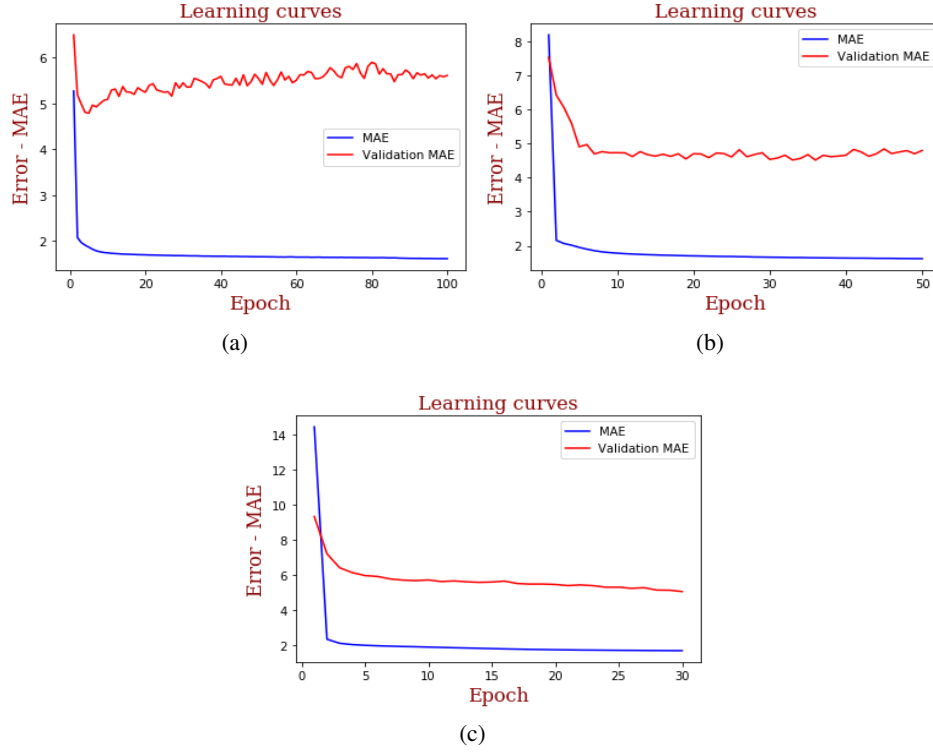


Figure 12: in (a), (b), and (c), we have learning curves for: 256 units/hidden layer, batch size of 64 and 100 epochs; 256 units/hidden layer, batch size of 128 and 50 epochs; and 256 units/hidden layer, batch size of 256, and 30 epochs, respectively.

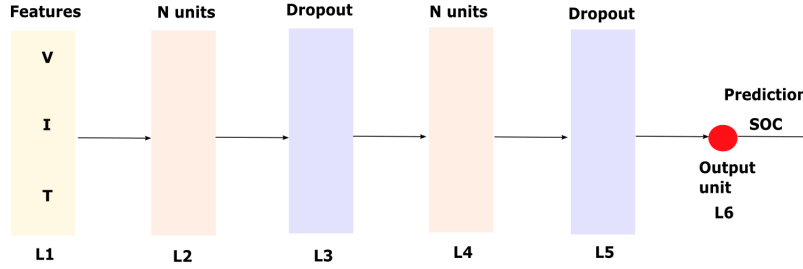


Figure 13: DFN with six (6) layers.

However, as indicated by the learning curves in Fig. 14, the DFN model with four hidden layers (two pairs of a 256 units/hidden layer followed by a dropout layer with a dropout rate of 0.5) has a greater power of generalization than the previous model. The MAE obtained on the test set was approximately 2.0% in this case.

4 Conclusions

This paper presents two simple DFN models with two and four hidden layers, respectively, using an optimizer with adaptive learning rules, and the Relu activation function, in order to estimate the State of Charge (SOC) of a Panasonic 18650PF lithium-ion battery of the Neural Network (NN) drive cycle of dataset [55] using the K-fold cross-validation method.

The DFN model with four hidden layers presents a better power of generalization, not only because it has a greater capacity in terms of more layers, but also due to the application of additional regularization techniques such as dropout

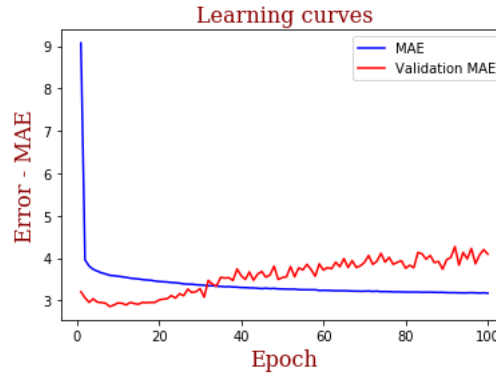


Figure 14: learning curves for a model with 256 units/hidden layer, batch size of 128, dropout rate of 0.5.

layers and parameter norm penalties. The contribution of this work is to present a methodology of building a DFN for a lithium-ion battery and its performance assessment, which follows the best practices in machine learning.

References

- [1] S. N. Laboratories, “DOE/EPRI 2013 electricity storage handbook in collaboration with NRECA,” Sandia National Laboratories, USA, Tech. Rep., 2013.
- [2] M. A. Hannan and et al., “Review of Energy Storage Systems for Electric Storage Vehicle Applications: Issues and Challenges,” *Renewable and Sustainable Energy Reviews*, vol. Vol. 69, pp. 771 – 789, 2016.
- [3] M. S. Whittingham, “History, Evolution, and Future Status of Energy Storage,” *Proceedings of the IEEE*, vol. Vol. 100, pp. 1518 – 1534, 2012.
- [4] X. Luo and et al., “Overview of Current Development in Electrical Energy Storage Technologies and the Application Potential in Power System Operation,” *Applied Energy*, vol. Vol. 137, pp. 511 – 536, 2015.
- [5] R. H. Byrne and et al., “Energy Management and Optimization Methods for Grid Energy Storage Systems,” *IEEE ACCESS*, 2017.
- [6] S. N. Motapon and et al., “A Generic Electrothermal Li-ion Battery Model for Rapid Evaluation of Cell Temperature Temporal Evolution,” *IEEE Transactions on Industrial Electronics*, vol. Vol. 64, no. 2, pp. 998 – 1007, February 2017.
- [7] T. Huria and et al., “High fidelity electrical model with thermal dependence for characterization and simulation of high power lithium battery cells,” in *IEEE International Electric Vehicle Conference*. IEEE, 2012.
- [8] L. Ren and et al., “Remaining useful life prediction for lithium-ion battery: A deep learning approach,” *IEEE ACCESS*, vol. 6, pp. 50 587–50 598, 2018.
- [9] D. H. Jeon, “Numerical Modeling of Lithium Ion Battery for Predicting Thermal Behavior in a Cylindrical Cell,” *Current Appl. Phys.*, vol. Vol. 14, no. 2, pp. 196 – 205, Feb. 2014.
- [10] J. Li and et al., “An Electrochemical-Thermal Model Based on Dynamics Responses for Lithium Iron Phosphate Battery,” *J. Power Sources*, vol. Vol. 255, pp. 130 – 143, June 2014.
- [11] R. Zhao, P. J. Kollmeyer, R. D. Lorenz, and T. M. Jahns, “A compact unified methodology via a recurrent neural network for accurate modeling of lithium-ion battery voltage and state-of-charge,” in *2017 IEEE Energy Conversion Congress and Exposition (ECCE)*, 2017, pp. 5234–5241.
- [12] E. Chemali and et al., “State-of-charge estimation of li-ion batteries using deep neural networks: a machine learning approach,” *Journal of Power Sources*, vol. 400, pp. 242–255, 2018.
- [13] B. Chen, T. Medini, and A. Shrivastava, “SLIDE: In Defense of Smart Algorithms over Hardware Acceleration for Large-Scale Deep Learning Systems,” *arXiv*, march 2019.
- [14] I. GoodFellow, Y. Bengio, and A. Courville, *Deep Learning*, 1st ed. MIT Press, 2016.
- [15] Y. LeCun, Y. Bengio, and G. Hinton, “Deep learning,” *Nature*, vol. 521, pp. 436–444, 2015.

- [16] S. Mallat, "Understanding deep convolutional networks," *Phil. Trans. R. Soc. A*, 2016. [Online]. Available: <http://rsta.royalsocietypublishing.org>
- [17] S. Minaee and A. A. Abdolrashidi, "Deep-emotion: Facial expression recognition using attentional convolutional network," *arXiv*, february 2019. [Online]. Available: <http://arxiv.org/abs/1902.01019>
- [18] D. Silver and et. al., "Mastering chess and shogi by self-play with a general reinforcement learning algorithm," *Science*, vol. 362, pp. 1140–1144, dec. 2018.
- [19] E. Chemali, P. J. Kollmeyer, M. Preindl, R. Ahmed, and A. Emadi, "Long short-term memory networks for accurate state-of-charge estimation of li-ion batteries," *IEEE Transactions on Industrial Electronics*, vol. 65, no. 8, pp. 6730–6739, 2018.
- [20] P. Kollmeyer, A. Hackl, and A. Emadi, "Li-ion battery model performance for automotive drive cycles with current pulse and eis parameterization," in *2017 IEEE Transportation Electrification Conference and Expo (ITEC)*, 2017, pp. 486–492.
- [21] S. Sepasi, R. Ghorbani, and B. Y. Liaw, "Improved extended kalman filter for state of charge estimation of battery pack," *Journal of Power Sources*, vol. 255, pp. 368–376, 2014.
- [22] M. Charkhgard and M. Farrokhi, "State-of-charge estimation for lithium-ion batteries using neural networks and ekf," *IEEE Transactions on Industrial Electronics*, vol. 57, dec. 2010.
- [23] J. Du, Z. Liu, and Y. Wang, "State of charge estimation for li-ion battery based on model from extreme learning machine," *Control Engineering Practice*, vol. 26, pp. 11–19, 2014.
- [24] Y.-S. Lee, W.-Y. Wang, and T.-Y. Kuo, "Soft computing for battery state-of-charge (bsoc) estimation in battery string systems," *IEEE Transactions on Industrial Electronics*, vol. 55, no. 1, jan. 2014.
- [25] W.-Y. Chang, "Estimation of the state of charge for a lfp battery using a hybrid method that combines a rnn neural network, an ols algorithm and aga," *Electrical Power and Energy Systems*, vol. 53, pp. 603–611, 2013.
- [26] F. Chollet, *Deep Learning with Python*, 1st ed. Manning Publications, 2018.
- [27] K. P. Murphy, *Machine Learning: A Probabilistic Approach*. The MIT Press, 2012.
- [28] R. Anderson et al, "Chapter I – Introduction," in *The Handbook of Artificial Intelligence*, A. Barr and E. A. Feigenbaum, Eds., vol. 1. Elsevier, 1981.
- [29] M. A. Boden, *AI Its Nature and Future*, 1st ed. Oxford University Press, 2016.
- [30] W. S. McCulloch and W. Pitts, "A logical calculus of the ideas immanent in nervous activity," *Bulletin of Mathematical Biophysics*, vol. 5, pp. 115–133, 1943. [Online]. Available: <http://www.cs.cmu.edu/~epxing/Class/10715/reading/McCulloch.and.Pitts.pdf>
- [31] A. M. Turing, "On Computable Numbers, with an Application to the Entscheidungsproblem," *Proceedings of the London Mathematical Society*, vol. 42, pp. 230–265, 1936.
- [32] S. Russel and P. Norvig, *Inteligência Artificial*, terceira ed. ed. Rio de Janeiro: Elsevier, 2013. [Online]. Available: <http://aima.cs.berkeley.edu/>
- [33] G. Cybenko, "Approximation by superpositions of a sigmoidal function," *Math. Control Signal Systems*, vol. 2, pp. 303–314, 1989. [Online]. Available: <https://doi.org/10.1007/BF02551274>
- [34] A. V. Oppenheim and R. W. Schaffer, *Discrete-Time Signal Processing*, 3rd ed. Pearson, 2009.
- [35] B. P. Lathi, *Signal Processing and Linear Systems*. Oxford University Press, 1998.
- [36] A. Newell, "Physical symbol systems," *Cognitive Science*, vol. 4, pp. 135–183, April–June 1980.
- [37] ACM, "A. M. Turing Award 2018," <https://awards.acm.org/about/2018-turing>, 2020.
- [38] L. Cun, B. Boser, J. S. Denker, D. Henderson, R. E. Howard, W. Hubbard, and L. D. Jackel, "Handwritten Digit Recognition with a Back-Propagation Network," in *Advances in Neural Information Processing Systems*. Morgan Kaufmann, 1990, pp. 396–404.
- [39] J. McCarthy and E. A. Feigenbaum, "In Memoriam: Arthur Samuel: Pioneer in Machine Learning," *AI Magazine*, vol. 11, no. 3, p. 10, Sep. 1990. [Online]. Available: <https://www.aaai.org/ojs/index.php/aimagazine/article/view/840>
- [40] A. L. Samuel, "Some Studies in Machine Learning Using the Game of Checkers," *IBM Journal of Research and Development*, vol. 3, no. 3, pp. 210–229, 1959.
- [41] W. Ertel, *Introduction to Artificial Intelligence*, 2nd ed. Springer, 2017.
- [42] T. M. Mitchell, *Machine Learning*. McGraw-Hill Dscience/Eng./Math, 1997.

- [43] D. Silver and et al, “General Reinforcement Learning Algorithm,” *arXiv*, 2017. [Online]. Available: https://arxiv.org/pdf/1712.01815.pdf?utm_campaign=nathan.ai%20newsletter&utm_medium=email&utm_source=Revue%20newsletter
- [44] B. Widrow and M. E. Hoff, “Adaptive switching circuits,” *IRE WESCON Convention Record*, pp. 96–104, 1960.
- [45] F. Rosenblatt, “The Perceptron: a probabilistic model for information storage and organization in the brain,” *Psychological Review*, vol. 65, pp. 386–408, 1958.
- [46] D. E. Rumelhart, G. E. Hinton, and J. W. Ronald, “Learning Internal Representations by Error Propagation,” in *Parallel Distributed Processing: Explorations in The Microstructure of Cognition*, D. E. Rumelhart and J. L. McClelland, Eds., vol. 1. Foundations, Cambridge, MA: Bradford Books/MIT Press, 1986.
- [47] A. E. B. Jr. and Y. C. Ho, *Applied Optimal Control*. Blaisdell, 1969.
- [48] P. J. Werbos, “Beyond Regression: New tools for prediction and analysis in the behavioral sciences,” 1974.
- [49] D. B. Parker, “Learning Logic,” Center for Computational Research in Economics and Management Science, MIT, 1985.
- [50] Y. LeCun, “A Learning Scheme for Asymmetric Threshold Network,” in *Disordered systems and biological organization*, E. Bienenstock, F. Fogelman, and G. Weisbuch, Eds. Springer Verlag, 1986.
- [51] A. Papoulis, *Probability, Random Variables, and Stochastic Processes*, 3rd ed. McGraw-Hill, 1996.
- [52] D. H. Wolpert, “The Lack of A Priori Disctintions Between Learning Algorithms,” *Neural Computation*, vol. 8, pp. 1341–1390, 1996.
- [53] G. E. Hinton, S. Osindero, and Y. Teh, “A fast learning algorithm for deep belief nets,” *Neural Computation*, vol. 18, pp. 1527–1554, 2006.
- [54] F. Chollet and J. J. Allaire, *Deep Learning with R*, 1st ed. Manning Publications, 2017.
- [55] P. Kollmeyer, “Panasonic 18650PF Li-ion Battery Data,” *Mendeley Data*, vol. 1, 2018. [Online]. Available: <https://data.mendeley.com/datasets/wykht8y7tg/1>
- [56] A. Gulli, A. Kapoor, and S. Pal, *Deep Learning with TensorFlow 2 and Keras*, 2nd ed. Packt>, 2019.
- [57] S. Skansi, *Introduction to Deep Learning: From Logical Calculus to Artificial Intelligence*, 1st ed. Springer, 2018.
- [58] Google, “Tensorflow,” 2020. [Online]. Available: <https://www.tensorflow.org/?hl=pt-br>
- [59] A. Paszke, S. Gross, S. Chintala, and G. Chanan, “Pytorch,” 2020. [Online]. Available: <https://pytorch.org>
- [60] Apache, “MXNet,” 2020. [Online]. Available: <https://mxnet.apache.org>
- [61] Microsoft, “Microsoft Cognitive Toolkit,” 2020. [Online]. Available: <https://docs.microsoft.com/en-us/cognitive-toolkit/>
- [62] Facebook, “Caffe2,” 2020. [Online]. Available: <https://caffe2.ai>
- [63] Google, “Colaboratory,” 2020. [Online]. Available: <https://colab.research.google.com/notebooks/intro.ipynb>